Negative refraction observed in a metallic ferromagnet in the gigahertz frequency range

Andrei Pimenov, Alois Loidl, K. Gehrke, V. Moshnyaga, Konrad Samwer

Angaben zur Veröffentlichung / Publication details:

Pimenov, Andrei, Alois Loidl, K. Gehrke, V. Moshnyaga, and Konrad Samwer. 2007. "Negative refraction observed in a metallic ferromagnet in the gigahertz frequency range." Physical Review Letters 98 (19): 197401. https://doi.org/10.1103/physrevlett.98.197401.

Negative Refraction Observed in a Metallic Ferromagnet in the Gigahertz Frequency Range

A. Pimenov,[1,2] A. Loidl,[2] K. Gehrke,[3] V. Moshnyaga,[3] and K. Samwer[3]

[1]*Experimentelle Physik IV, Universität Würzburg, 97074 Würzburg, Germany*

[2]*Experimentalphysik V, Center for Electronic Correlations and Magnetism, Universität Augsburg, 86135 Augsburg, Germany*

[3]*I. Physikalisches Institut, Universität Göttingen, 37073 Göttingen, Germany*

(Received 10 November 2006; published 10 May 2007)

It is generally believed that nature does not provide materials with negative refraction. Here we demonstrate experimentally that such materials do exist at least at GHz frequencies: ferromagnetic metals reveal a negative refraction index close to the frequency of the ferromagnetic resonance. The experimental realization utilizes a colossal magnetoresistance manganite $La_{2/3}Ca_{1/3}MnO_3$ as an example. In this material the negative refractive index can be achieved even at room temperature using external magnetic fields.

DOI: 10.1103/PhysRevLett.98.197401 PACS numbers: 78.20.Ci, 41.20.Jb, 75.47.Lx, 76.50.+g

Materials with a negative refractive index reverse our understanding of modern optics. In a negative refraction material (NRM) the phase of the electromagnetic wave propagates in a direction opposite to the energy flow. In 1968 Veselago [1] proposed that a material with simultaneously negative electric permittivity $\varepsilon < 0$ and negative magnetic permeability $\mu < 0$ would reveal a negative refractive index. Only recently could this prediction be confirmed experimentally [2–7]. Lenses designed from the materials with negative refraction can be constructed with flat surfaces and, most importantly, they reveal a resolution beyond the diffraction limit [8]. This superlensing effect has been experimentally verified for a number of metamaterials at microwave frequencies [9,10], and even for optical frequencies [11] although the latter did not utilize the negative refraction material. The superlensing effect which uses negative refraction suffers strongly from residual losses [12]. In addition, the original idea [8] requires that both permittivity and permeability equal to minus one. The dielectric permittivity of metals is negative below plasma frequency and the first condition can be fulfilled even for visible light. On the contrary, magnetic permeability of known magnetic materials approaches unity already above terahertz frequencies [13]. Therefore the search for magnetic systems with $\mu = -1$ up to the optical range remains an actual task.

It is generally believed that nature does not provide materials with negative refraction [13] and hence, metamaterials [2–5], photonic crystals [6,7,14], or multilayers [15,16], have been utilized as NRMs. In this Letter we demonstrate that natural materials with negative refraction do exist at least at GHz frequencies. Indeed, a good metal would reveal negative permittivity and, if it is simultaneously ferromagnetic, negative magnetic permeability close to magnetic resonance can be realized as well [13]. Even more, the requirement of perfect metallic conductivity is not stringent. The complex dielectric permittivity (ε^*) of metals can be written as $\varepsilon^* = \varepsilon_1 + i\varepsilon_2 = \varepsilon_1 + i\sigma/\varepsilon_0\omega$, where $\varepsilon_1 = \mathrm{Re}(\varepsilon^*)$ is the real part of the permittivity, σ is the conductivity, $\omega = 2\pi\nu$ is the angular frequency, and ε_0 is the permittivity of free space. For metals at not too high frequencies an inequality holds: $|\varepsilon_1| \ll \varepsilon_2$. Therefore, in a good approximation the permittivity of a metal is purely imaginary and the border between good metals with $\varepsilon_1 < 0$ and bad metals with $\varepsilon_1 > 0$ is rather subtle. As has been shown theoretically [17], the full condition to obtain negative refraction is slightly broader than Veselago's criterion and can be written as [18]

$$(\varepsilon_1 + |\varepsilon^*|)(\mu_1 + |\mu^*|) < \varepsilon_2\mu_2. \quad (1)$$

Here μ_1 and μ_2 are real and imaginary parts of the complex magnetic permeability $\mu^* = \mu_1 + i\mu_2$. In case of a metal $|\varepsilon^*| \approx \varepsilon_2$ and Eq. (1) is simplified to

$$\mu_1 < 0,$$

which is now a final condition applied to ferromagnetic metals. For an isotropic ferromagnet the magnetic contribution of the ferromagnetic resonance (i.e., the strength of the mode) can be written as $\Delta\mu = 4\pi M_0/H_r$, where M_0 is the static magnetization and H_r is the resonance field. For a typical ferromagnet $4\pi\mu_0 M_0 \sim 1$ T, which leads to $\Delta\mu \sim 1$ at gigahertz frequencies ($\mu_0 H_r \sim 1$ T). Here μ_0 is the permeability of free space. For narrow ferromagnetic modes the magnetic permeability can therefore easily reach negative values close to the resonance.

To demonstrate that negative refraction can be obtained in a bulk metallic ferromagnet, we choose $La_{2/3}Ca_{1/3}MnO_3$ (LCMO), a material from the family of colossal magnetoresistance manganites [19,20]. This is a well studied system with the phase diagram allowing the tuning of the conducting and magnetic properties between antiferromagnetic insulator to ferromagnetic metal. Close to $Ca_{1/3}$ doping LCMO reveals a metallic ferromagnetic state with a strong mode of the ferromagnetic resonance. These properties make LCMO an ideal candidate to test the existence of negative refraction in ferromagnetic metals. In addition, the preparation procedure of manganites is well established and the samples of high quality can be easily grown using various techniques. In the present case, LCMO films with a typical thickness of 550 nm were prepared on MgO substrates by a metalorganic aerosol

deposition [21]. Because of high refractive index of LCMO the wavelength of the GHz radiation within the sample $\lambda/n \sim 5\ \mu$m is about 1 order of magnitude larger than the film thickness.

The dynamic experiments for frequencies 60 GHz $< \nu <$ 380 GHz were carried out in a Mach-Zehnder interferometer arrangement [22,23] which allows both the measurements of the transmittance and the phase shift of a plane-parallel sample. The frequency-dependent transmission spectra are analyzed using the Fresnel formulas for the transmittance $T = |t|^2$ [23,24]

$$t = \frac{(1-r^2)t_1}{1-r^2t_1^2}, \quad \text{where } r = \frac{\sqrt{\varepsilon/\mu}-1}{\sqrt{\varepsilon/\mu}+1} \quad \text{and} \quad t_1 = \exp(-2\pi i\sqrt{\varepsilon\mu}d/\lambda). \tag{2}$$

Here r is the reflection amplitude at the air-sample interface, t_1 is the "pure" transmission amplitude, ε and μ are the (complex) dielectric permittivity and magnetic permeability of the sample, respectively, d is the sample thickness, and λ is the radiation wavelength. Equation (2) is valid for both thin and thick samples and can be easily extended to include the properties of the substrate [24].

Figure 1 shows the conductivity of LCMO as function of temperature in a zero magnetic field compared to the data in a static field of $\mu_0 H = 5$ T. A sharp metal-to-insulator transition is observed without magnetic field, which corresponds to the magnetic transition from the paramagnetic to the ferromagnetic state. This correlates well with the magnetic moment of LCMO shown in Fig. 1. In the presence of external magnetic fields the transition temperature strongly increases and broadens. As documented in Fig. 1, in the external field of $\mu_0 H = 5$ T the ferromagnetic and metallic state persists even at room temperature. The absolute values of conductivity range from 100 to 1000 $\Omega^{-1}\,\mathrm{cm}^{-1}$, which corresponds to a large imaginary part of the dielectric permittivity $\mathrm{Im}(\varepsilon^*) = \varepsilon_2$ between 1.2×10^3 and 1.2×10^4, respectively. In the presence of this large imaginary part, the real part of the permittivity cannot be measured accurately in the gigahertz range and can only be estimated as $(2 \pm 1) \times 10^2$. However, the complex refractive index $n^* = n + i\kappa = \sqrt{\varepsilon^*\mu^*}$ is dominated by the large $\mathrm{Im}(\varepsilon^*)$ and the resulting errors are below 5%.

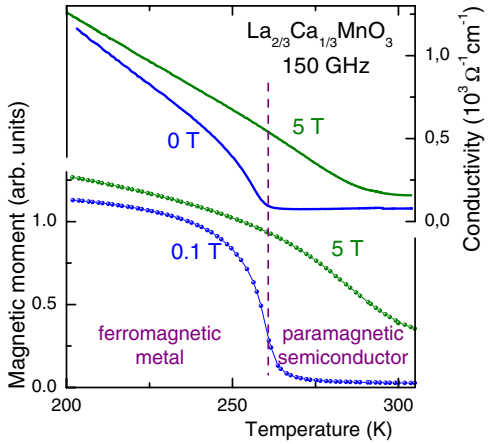

FIG. 1 (color online). Temperature dependence of the conductivity and magnetization of the LCMO film. Left scale: Magnetic moment of LCMO for different magnetic fields. Right scale: conductivity at $\nu = 150$ GHz without magnetic field (blue) and in an external field of $\mu_0 H = 5$ T (green). Dashed line indicates the border between ferromagnetic metallic and paramagnetic semiconducting phases.

To separate dielectric and magnetic contributions of LCMO two experimental geometries of the transmittance experiment have been used, $\tilde{h} \perp \mu_0 H$ and $\tilde{h} \parallel \mu_0 H$. Here $\tilde{h}$ is the ac magnetic field of the electromagnetic wave and H is the static field. The experimental arrangements are shown schematically in the inset of Fig. 2. The excitation of the magnetic resonance and, therefore, the nonzero magnetic susceptibility can be realized in the geometry $\tilde{h} \perp \mu_0 H$ only [25]. This follows from the solution of the Bloch's equations for the motion of the magnetic moments in an external field. The nonzero magnetic susceptibility arises due to the term $\tilde{h} \times M_0$. These conditions are demonstrated experimentally in Fig. 2, which shows transmittance and phase shift of LCMO for two complementary experimental geometries. The red curves show the "nonmagnetic" data with $\tilde{h} \parallel \mu_0 H$ and the black curves represent the geometry with $\tilde{h} \perp \mu_0 H$, where the ferromagnetic resonance is excited. Combining the results of both experi-

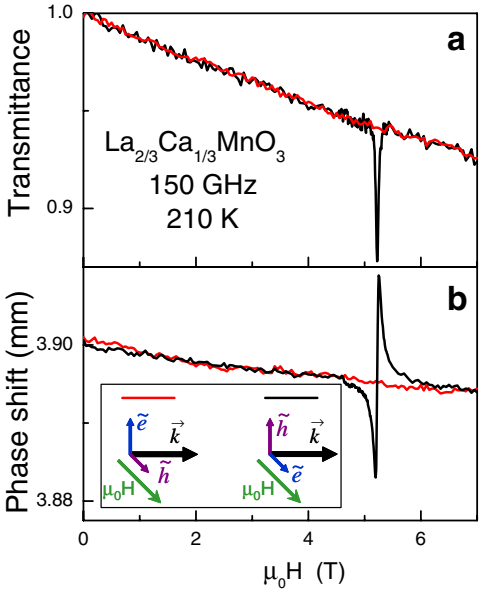

FIG. 2 (color online). Complex transmittance of LCMO within two possible experimental geometries. (a) Amplitude of the transmission coefficient for magnetic ($\tilde{h} \perp \mu_0 H$, black curve) and nonmagnetic ($\tilde{h} \parallel \mu_0 H$, red curve) geometries. (b) Phase shift of the transmittance. The notations are the same as in (a). The inset represents the experimental geometries. Here the wave vector $\vec{k}$ gives the propagation direction, $\mu_0 H$ is the external magnetic field, and $\tilde{e}$ and $\tilde{h}$ are the ac electric and magnetic fields of the electromagnetic wave, respectively.

ments the dielectric permittivity and magnetic permeability can be obtained independently. Within the geometry $\tilde{h} \parallel \mu_0 H$ *no magnetic contribution exists* and $\mu = 1$. Therefore, the dielectric permittivity can be calculated from transmittance and phase shift of this geometry. Combining these data with the results obtained within the geometry $\tilde{h} \perp \mu_0 H$ the magnetic permeability is calculated. Finally, the complex refractive index is calculated via $n^* = \sqrt{\varepsilon^* \mu^*}$. We note that due to continuous variation of the refractive index by the external magnetic field the sign of the square root is solved automatically. Typical field dependencies of the dielectric permittivity and the magnetic permeability of LCMO are given in Fig. 3. These data have been obtained from the transmittance and phase shift of Fig. 2 using Eq. (2). Here the changes in the dielectric permittivity correlate well with the results in Fig. 1 and represent the gigahertz magnetoresistance in LCMO.

Figure 4 represents the magnetic field dependence of the refractive index (a) and the absorption coefficient (b) of LCMO at a frequency of 150 GHz and as function of magnetic field close to the ferromagnetic resonance in this compound. Closely similar field dependencies have been observed for frequency of 90 GHz except that the resonance position is roughly 3.1 T in this case. With increasing temperature the resonance position shifts to higher magnetic fields. This behavior agrees well with the decrease of the ferromagnetic moment in LCMO (Fig. 1) and corresponds to the $\mu_0 H \perp \vec{k}$ geometry of the experiment (Voigt geometry [26]). Within this geometry the static magnetic field lies within the sample plane and the resonance frequency is given by $\omega_r = \gamma\sqrt{(H + 4\pi M)H}$, where γ is the gyromagnetic ratio. According to this expression and in the ferromagnetic state the resonance field is shifted to lower fields approximately proportional to the static magnetization. Figure 4 clearly documents that a large field region with negative refraction exists especially in the ferromagnetic metallic state. In addition, the inset in Fig. 4 shows the refractive index of LCMO in a complex scale using the magnetic field as parameter. The region with negative refraction is shown as the hatched area in the inset.

Although the presented results demonstrate the possibility of negative refraction in a bulk material, the applications, e.g., towards the superlensing effect remain restricted. The basic problems to be solved are the losses in the ferromagnets close to the resonance and the anisotropy of the magnetic permeability. To suppress the losses a ferromagnetic material with a very narrow resonance line may provide a reasonable solution. The anisotropy of the permeability and, therefore, of the refractive index, cannot be removed within the present geometry. The sensitivity to the polarization of the incident radiation is suppressed in the Faraday geometry, where static magnetic fields are perpendicular to the sample surface and cylindrical symmetry exits. To reduce the anisotropy for different incident angles further experimental efforts are necessary.

Finally, Fig. 5 compares the lowest values of the refractive index, obtained in this experiment, for two different frequencies. The lowest value of the refractive index remains negative in the full range of the present experiment

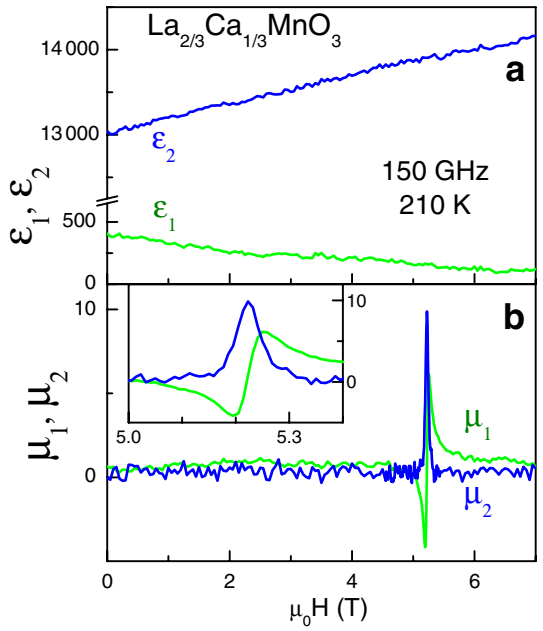

FIG. 3 (color online). Magnetic field-dependence of the dielectric permittivity (a) and magnetic permeability (b) of LCMO at $\nu = 150$ GHz and $T = 210$ K. Green curves—real parts, blue curves—imaginary parts. The inset shows the magnetic permeability in the vicinity of the resonance field.

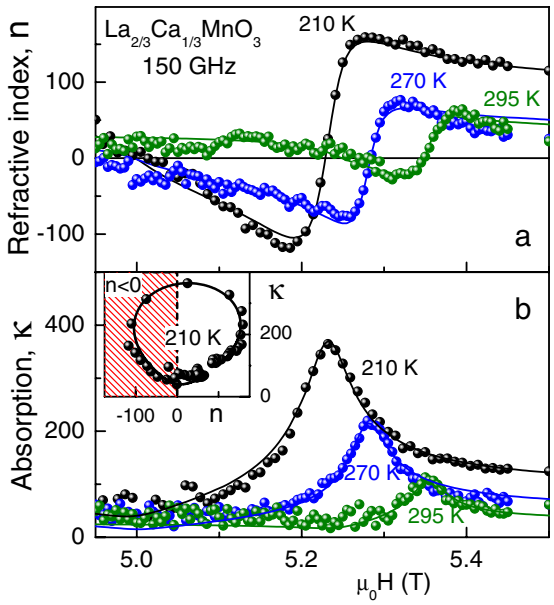

FIG. 4 (color online). Magnetic field dependence of the refractive index (a) and absorption coefficient (b) of LCMO at $\nu = 150$ GHz and for different temperatures. Symbols—experiment, lines—fits to the Lorentz form of the ferromagnetic resonance. The inset presents the refractive index at $T = 210$ K on the complex scale.

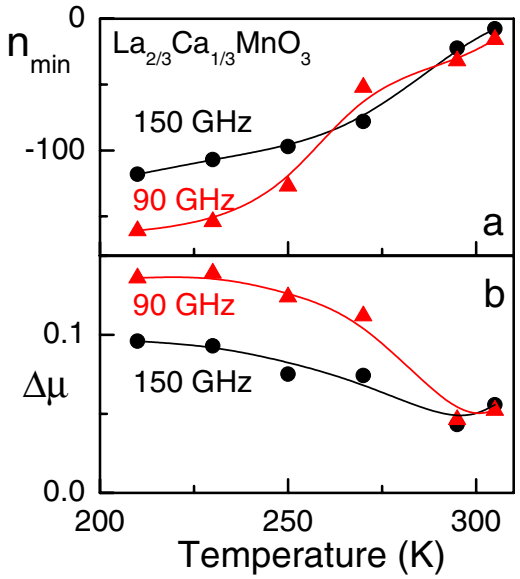

FIG. 5 (color online). (a) Lowest experimentally achieved value of the refractive index at two frequencies of the experiment. (b) Strength of the ferromagnetic mode obtained from the Lorentz fits. Symbols represent experimental data; lines are guides to the eye.

210 K $\leq T \leq$ 305 K. The available values of the refractive index correlate well with the strength of the magnetic mode [Fig. 5(b)] and with the static magnetization (Fig. 1), which is an expected behavior of a classical ferromagnet. Of course for modern optoelectronic applications the problem remains to provide negative refraction in ferromagnetic films for visible light. Negative dielectric permittivity is a characteristic of many metals at optical frequencies. However, negative magnetic permeability is restricted close to ferromagnetic resonance in the mm wavelength range and fades away towards higher frequencies [13]. In addition, we cannot exclude that an electronic phase separation, which has been shown to be important in manganites [27], plays a role in constituting negative refraction.

In conclusion, we have shown experimentally that the conditions for negative refraction can be realized in metallic ferromagnets. In the present work, the negative refraction index has been obtained in the colossal magnetoresistance material $La_{2/3}Ca_{1/3}MnO_3$ and in the gigahertz frequency range. Using two different experimental geometries, the magnetic permeability and dielectric permittivity have been obtained independently to demonstrate the negative refraction close to the ferromagnetic resonance. In principle, similar effects can be expected in any ferromagnetic metal such as iron, provided the existence of narrow ferromagnetic resonance.

[1] V. G. Veselago, Sov. Phys. Usp. **10**, 509 (1968).
[2] D. R. Smith, W. J. Padilla, D. C. Vier, S. C. Nemat-Nasser, and S. Schultz, Phys. Rev. Lett. **84**, 4184 (2000).
[3] R. A. Shelby, D. R. Smith, and S. Schultz, Science **292**, 77 (2001).
[4] C. G. Parazzoli, R. B. Greegor, K. Li, B. E. C. Koltenbah, and M. Tanielian, Phys. Rev. Lett. **90**, 107401 (2003).
[5] A. A. Houck, J. B. Brock, and I. L. Chuang, Phys. Rev. Lett. **90**, 137401 (2003).
[6] S. Foteinopoulou, E. N. Economou, and C. M. Soukoulis, Phys. Rev. Lett. **90**, 107402 (2003).
[7] E. Cubukcu, K. Aydin, E. Ozbay, S. Foteinopoulou, and C. M. Soukoulis, Nature (London) **423**, 604 (2003).
[8] J. B. Pendry, Phys. Rev. Lett. **85**, 3966 (2000).
[9] A. N. Lagarkov and V. N. Kissel, Phys. Rev. Lett. **92**, 077401 (2004).
[10] A. Grbic and G. V. Eleftheriades, Phys. Rev. Lett. **92**, 117403 (2004).
[11] N. Fang, H. Lee, C. Sun, and X. Zhang, Science **308**, 534 (2005).
[12] N. Garcia and M. Nieto-Vesperinas, Phys. Rev. Lett. **88**, 207403 (2002).
[13] J. B. Pendry and D. R. Smith, Phys. Today **57**, No. 6, 37 (2004).
[14] P. V. Parimi, W. T. Lu, P. Vodo, and S. Sridhar, Nature (London) **426**, 404 (2003).
[15] A. Pimenov, A. Loidl, P. Przyslupski, and B. Dabrowski, Phys. Rev. Lett. **95**, 247009 (2005).
[16] A. Alù and N. Engheta, IEEE Trans. Antennas Propag. **51**, 2558 (2003); J. Appl. Phys. **97**, 094310 (2005).
[17] M. W. McCall, A. Lakhtakia, and W. S. Weiglhofer, Eur. J. Phys. **23**, 353 (2002).
[18] A. D. Boardman, N. King, and L. Velasco, Electromagnetics **25**, 365 (2005).
[19] K. Chahara, T. Ohno, M. Kasai, and Y. Kozono, Appl. Phys. Lett. **63**, 1990 (1993); R. von Helmolt, J. Wecker, B. Holzapfel, L. Schultz, and K. Samwer, Phys. Rev. Lett. **71**, 2331 (1993); S. Jin, T. H. Tiefel, M. McCormack, R. A. Fastnacht, R. Ramesh, and L. H. Chen, Science **264**, 413 (1994).
[20] M. B. Salamon and M. Jaime, Rev. Mod. Phys. **73**, 583 (2001).
[21] V. Moshnyaga, I. Khoroshun, A. Sidorenko, P. Petrenko, A. Weidinger, M. Zeitler, B. Rauschenbach, R. Tidecks, and K. Samwer, Appl. Phys. Lett. **74**, 2842 (1999).
[22] A. A. Volkov, Yu. G. Goncharov, G. V. Kozlov, S. P. Lebedev, and A. M. Prochorov, Infrared Phys. **25**, 369 (1985).
[23] D. Ivannikov, M. Biberacher, H.-A. Krug von Nidda, A. Pimenov, A. Loidl, A. A. Mukhin, and A. M. Balbashov, Phys. Rev. B **65**, 214422 (2002).
[24] M. Born and E. Wolf, *Principles of Optics* (Pergamon, Oxford, 1986).
[25] A. Abragam and B. Bleaney, *Electron Paramagnetic Resonance of Transition Ions* (Dover, New York, 1970), p. 95.
[26] A. K. Zvezdin and V. A. Kotov, *Modern Magnetooptics and Magnetooptical Materials* (Institute of Physics Publ., Bristol, 1997).
[27] E. Dagotto, T. Hotta, and A. Moreo, Phys. Rep. **344**, 1 (2001).